The main revisions are marked in a yellow color in the text; some parts have been rewritten in a clearer way adding some paragraphs to facilitate the understanding of paper. For all presented cases, tables of measured and adopted parameters have been added as requested (vertical logs and values tables are provided).

Author's responses to Reviewers

Reviewer 1

Thank you for appreciating our work. Based on the revisions on a second reviewer, some improvements have been made to facilitate the understanding of the article. The revised version of paper is now available and we look forward to receiving your feedback.

Thank you.

Reviewer 2

Thank you for appreciating our work and for suggestions given to improve it. Taking in account your revisions, a new version of paper will be submitted.

The second part of abstract and the part 1 have been revised in order to provide a better understanding (especially authors' thesis).

The part 2 was rewritten in a clearer way trying to better explain parameters and assumptions of stability charts; a table with adopted values of Hoek&Brown failure criterion has been added with a detailed exposition on the choice of these parameters. Equations (of curves) are missing because the curves represent the result of a parametric study for a large number of ideal cavities with varying geometric and mechanical parameters (adopted equation of failure criterion of Hoek & Brown is omitted because widely explained in Perrotti et al. (2018)). Figure 2,3,4 have not been merged to avoid difficulty to interpret a single graph with 12 curves (note that, based on m_i parameter, the values on the y-axis of three graphs are very different from each other). However, the resolution of the figures has been improved.

The part 3 was rewritten in a clearer way: an introductive paragraph has been added in order to explain the choice of presented case studies. Each study case is now presented in a similar way and tables of measured and adopted parameters have been added as requested (vertical logs and values tables are provided). The figures of instability evidences, especially for three case of sinkhole, are necessary to better understand the causes that lead the collapse of quarries (i.e. crushing of pillars that lead an enlargement of L dimension).

The part 4 highlights that presented real cases are well suited to verification through stability charts; however, in order to provide a validation index, other study cases, together with those here presented, will be considered in a future paper.

The revised version of paper is now available and we look forward to receiving your feedback.

Thank you.

FEM-based stability charts for underground cavities in soft carbonate rocks: validation through case-study applications

Perrotti M.[1], Lollino P. [1], Fazio N.L. [1], Parise M. [1,2]

[1] CNR – IRPI, Bari, 70126, Italy
[2] Department of Earth and Geo-environmental Sciences, University of Bari "Aldo Moro", Bari, 70126 Italy

Abstract

The stability of man-made underground cavities in soft rocks interacting with overlying structures and infrastructures represents a challenging problem to be faced. Based upon the results of a large number of parametric two-dimensional (2D) finite-element analyses of ideal cases of underground cavities, accounting for the variability both cave geometrical features and rock mechanical properties, specific charts have been recently proposed in the literature to assess at a preliminary stage the stability of the cavities. The purpose of the present paper is to validate the efficacy of the stability charts by the application to several case studies of underground cavities, considering both quarries collapsed in the past and quarries still stable. The stability graphs proposed by Perrotti et al. (2018) can be useful to evaluate, in a preliminary way, a safety margin for cavities that have not reached failure and to catch indications about predisposition to local or general instability phenomena. Alternatively, for sinkholes already occurred, the graphs may be useful in identifying the conditions that led to the collapse highlighting the importance of some structural elements (as pillars and internal walls) on the overall stability of the quarry system.

1. Introduction

The presence of underground cavities as a result of past mining operations of soft rocks, to be used as building material, nowadays induces high risk conditions for those regions characterised by a large number of underground quarries and mines. In Apulia region (southern Italy), soft and very soft carbonate rocks as calcarenites of Pliocene or Pleistocene age, have been largely used (Parise 2010, 2012), especially in the last century, in many types of construction, so that a diffuse net of cavities, nowadays underlying urban areas and infrastructures, was excavated in the last century and abandoned afterwards. In recent years, several collapses affected some of these cavity systems, involving structures and roads located at the ground surface and, therefore, inducing high risk for human life and properties (Fiore and Parise 2013). These effects are caused by degradation processes of these rock materials as a consequence of weathering- or human-induced actions over time (Ciantia et al. 2015); as a consequence, the stability of the quarries may evolve after decades from the time of excavation, giving rise to local or global cave instabilities and failures.

The problem of assessing the stability of underground cavities in soft rocks is generally faced with approaches characterized by different levels of accuracy and reliability. Phenomenological and analytical approaches are generally chosen in the preliminary stage of the analysis to deduce if the rock mass is close to instability or not (Gesualdo et al. 2001; Fraldi and Guarracino 2009; Carter

2014). Later on, more deterministic and accurate approaches could be adopted, such as those based on numerical modelling (Goodings and Abdulla 2002; Ferrero et al. 2010; Parise and Lollino 2011; Castellanza et al. 2018). The last mentioned approach can be very useful nowadays, because three-dimensional studies can be carried out due to the availability of powerful numerical codes, which are capable of treating a wide range of problems related to the structural features of the rock mass examined (for both continuous or discontinuous rock masses). However, although remaining the most efficient way to dealing with stability problems at the specific site scale, sophisticated numerical techniques cannot be applied effectively to a large dataset of stability assessments because they require a large amount of detailed input data, which are not frequently available, and consequently they cannot be practically used for a preliminary evaluation. On the contrary, wide regions throughout the world (e.g. southern part of Italy) are characterized by a huge number of cavities affecting the underground environment, so that representative three-dimensional numerical analyses cannot be developed efficiently for all the case studies. For this reason, physically- or mechanically-based stability charts can be useful to provide a preliminary assessment on the stability of the underground system, as a function of the geometrical and mechanical parameters (Evangelista et al. 2003; Federico and Screpanti 2003; Suchowerska et al. 2012). It is worthwhile remarking that the use of stability graphs should be considered only as a preliminary stage of the complete procedure to be followed for the stability assessment (Castellanza et al. 2018, Fiore et al. 2018). Therefore, when a medium to high level of hazard comes out from the application of the charts here proposed, more detailed and site-specific investigations must necessarily be applied. Based upon the results of a large number of parametric two-dimensional (2D) finite-element analyses of ideal cases of underground cavities that considered variability of geometrical features and mechanical properties found for a large number of underground cavities excavated in soft carbonate rocks, Perrotti et al. (2018) have proposed specific charts to assess at a preliminary stage the cave stability and to evaluate a safety margin with respect to the occurrence of failure.

The purpose of this paper is to validate the efficacy of the aforementioned stability charts proposed by Perrotti and co-authors by means of the application to several case studies of underground cavities, either subjected to collapse in the past or still stable, based upon the geometrical features and the geomechanical parameters known for the case studies; stability charts were applied either to (i) cases of sinkhole or to (ii) cavities that have not reached the collapse; in the first case (i) they show the importance of specific structural elements as pillars and partitions on the stability of the entire system of quarries, while in the second case (ii) it is possible to assess the degree of susceptibility and predisposition to instability phenomena.

2. FEM-based underground cave stability charts

Perrotti and co-authors (2018) have proposed a two-dimensional finite element parametric study that account for ideal schemes of rectangular cavities, as shown in Figure 1, with variable geometrical parameters, as the cavity width (L), the cavity height (h) and the overburden thickness (t). A large set of 2D finite-element analyses were carried out using Plaxis-2D software in order to evaluate possible correlations between geometrical features of cavities and material strength parameters. The ranges of variation of these variables are consistent with the typical intervals of values observed for man-made Apulian underground quarries excavated in soft carbonate rocks, belonging to the Calcarenite di Gravina formation (Coviello et al. 2005; Andriani and Walsh 2010;

Ciantia et al. 2015). In particular, the cavity width, L, is assumed to vary in a range from 1 to 30 meters, the cavity height, h, in a range from 2 to 8 meters, and the overburden thickness, t, in a range from 2 to 10 meters. Additional 3D-FEM analyses were also performed to evaluate the effect of the rock confinement in the third direction, which, generally, results in increasing the stability of underground quarries with respect to the 2D analyses.

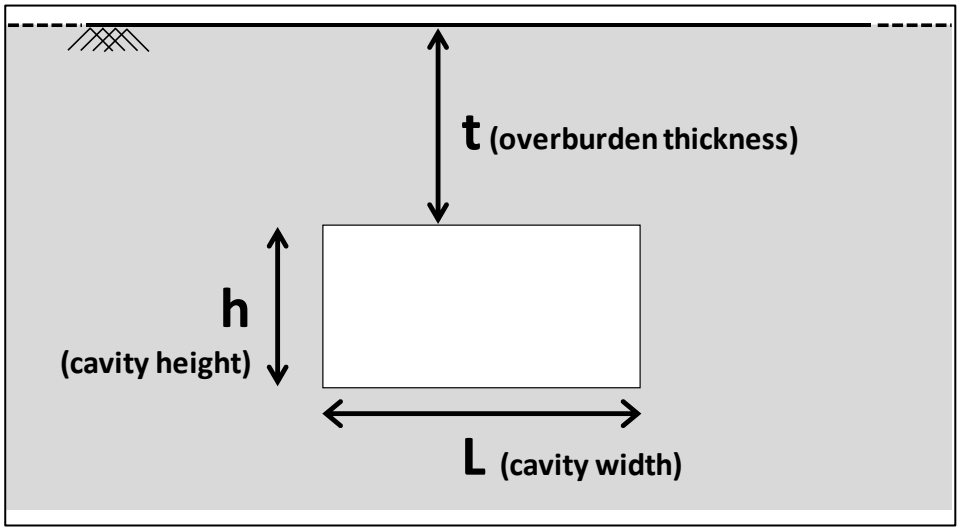

Figure 1. Geometrical parameters of the cavity (h = cavity height; L = cavity width; t = overburden thickness).

The mechanical behaviour of the soft and very soft carbonate rocks has been schematised according to an elastic perfectly plastic constitutive model characterized by a Hoek-Brown failure criterion (Hoek and Brown, 1997; Hoek and Martin, 2014), which is capable to simulate a nonlinear strength envelope in the Mohr's plane, as generally observed for calcarenite rocks; the main mechanical variable chosen in the parametric analyses was the value of uniaxial compressive strength σ_c ; threshold value $\sigma_{c,min}$ corresponds to the activation of a failure mechanism for the cavity calculated from 2D FEM analyses assuming the Hoek&Brown parameters reported in Table 1.

Parameter	σ_c	GSI (Geological Strenght Index)	m_i	D
Adopted value	variable	100	3 – 8 – 16	0

Table 1. Values of Hoek-Brown parameters assigned in 2D analyses.

The values of GSI, m_i and D have been chosen as follow.

Based upon field survey observations, which indicated that these rocks are rarely jointed, the rock mass was assumed to be intact and not affected by discontinuities, and consequently a geological strength index **GSI** (Hoek 1994) value equal to 100 was used in the analyses. It follows that the results obtained from the analyses cannot be considered valid for those cases where the rock mass is characterized by single joints or joint sets, so that the rock mass behaviour has a certain degree of anisotropy that cannot be disregarded.

The parameter $\mathbf{m_i}$ was defined, in first approximation, in accordance with the suggestions proposed by Cai (2010), to represent the ratio between the uniaxial compressive and tensile strength of the rock: three different values, equal to 3, 8 and 16 have been chosen in accordance with the values

proposed by Hoek (2007) for the specific rock type, as well as with the results of uniaxial compressive and tensile strength tests performed on samples belonging to different varieties of the Gravina Calcarenite Formation (Andriani and Walsh, 2010).

The parameter **D**, representative of the disturbance factor induced by the excavation technique, was prescribed equal to zero to simulate a rock mass that has not been disturbed or affected by stress release processes due to the specific hand-excavation technique adopted throughout the whole region (generally, this was the hand-excavation technique with chisels and hammers, adopted in order to obtain large blocks of calcarenites to be used as building material).

Fixed values of GSI and D, a large set of 2D FEM analyses was carried out for each of three values assumed for m_i . Parametric analyses allow to obtain resulting plots showing the $\sigma_{c,min}/\sigma_v$ ratio (i.e. threshold value of uniaxial compressive strength mobilized at failure divided by vertical stress before excavation, acting at the depth of the cavity roof) as a function of the non-dimensional ratio L/t, keeping fixed the non-dimensional cavity shape ratio L/h. Stability graphs are shown in Figures 2, 3 and 4, as referred to values of m_i equal, respectively, to 3, 8 and 16. The curves identify the stable area above the threshold curves. So, considering the value of m_i closest to the real value estimated for a specific cavity, is possible to enter one of three graphs with the ratios σ_c/σ_v and L/t (and following the curve of the non-dimensional cavity shape ratio L/h) estimated for a cavity to evaluate a safety margin with respect to failure. A point of a generic cavity that is on the line (or below this) is representative of a cavity with collapse already occurred. It should be pointed out that value of m_i greatly influences the results of the curves; in fact, the values on the y-axis of three graphs (Figure 2, 3 and 4) are very different from each other.

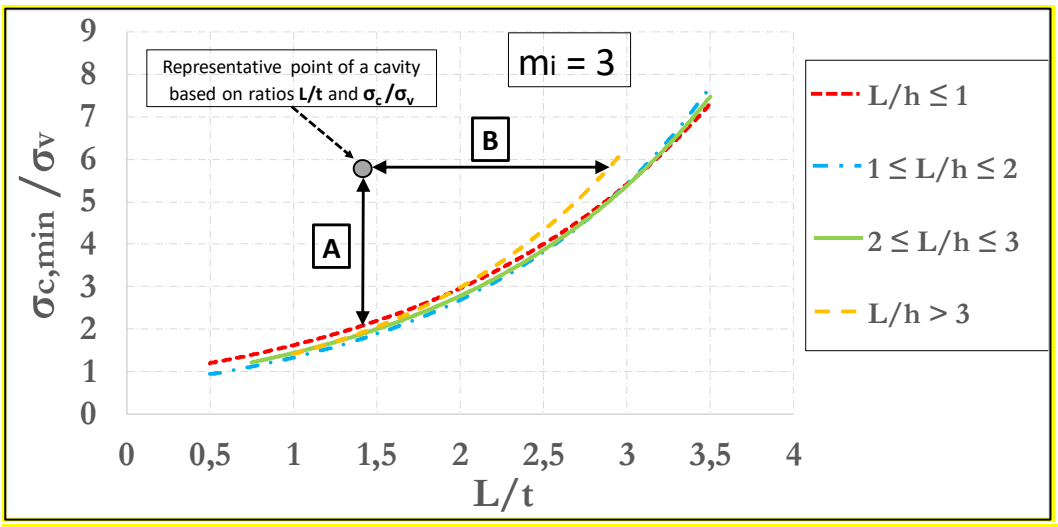

Figure 2. Curves of $\sigma_{c,min}/\sigma_v$ against L/t for different values of the ratio L/h (mi = 3) (modified after Perrotti et al. 2018).

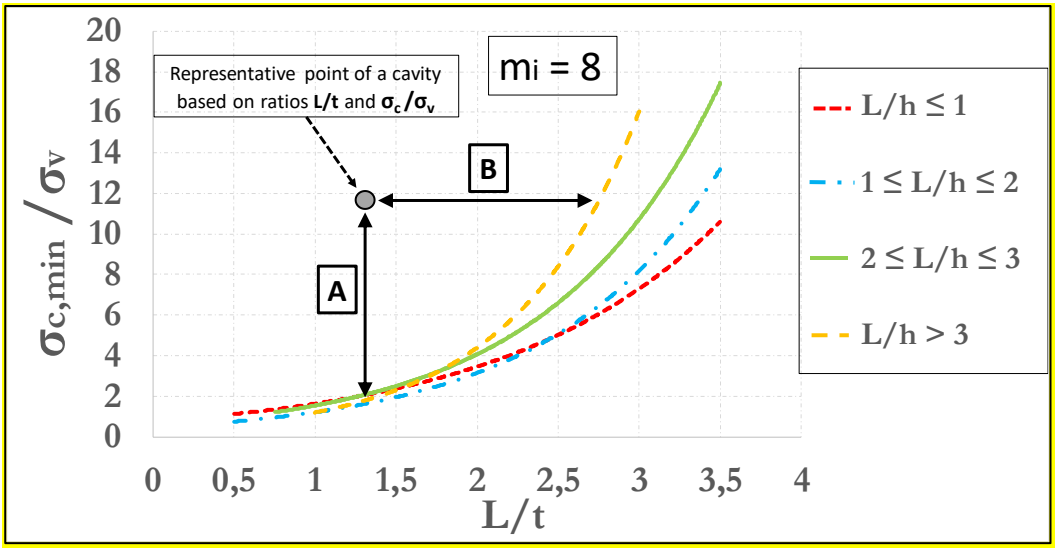

Figure 3. Curves of $\sigma_{c,min}/\sigma_v$ against L/t for different values of the ratio L/h (mi = 8) (modified after Perrotti et al. 2018).

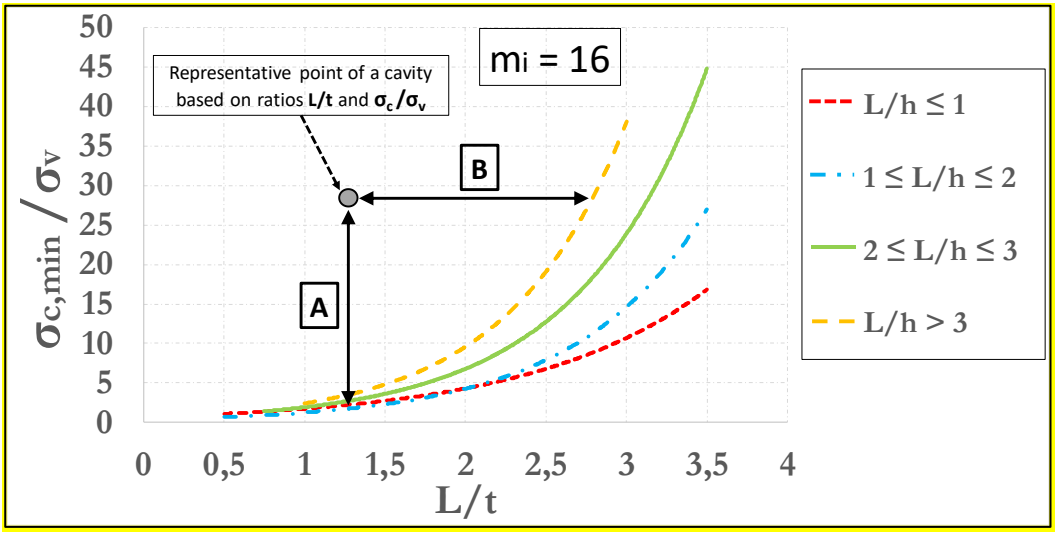

Figure 4. Curves of $\sigma_{c,min}/\sigma_v$ against L/t for different values of the ratio L/h (mi = 16) (modified after Perrotti et al. 2018).

These stability charts can be used to calculate the safety margin with respect to failure as the ratio between the actual in situ value of the rock uniaxial compressive strength (σ_c) and the threshold value for stability of the same parameter ($\sigma_{c,min}$) at the same L/t value (segment A in Figure 2, 3 and 4). Alternatively, the same plots allow to calculate the maximum value of the width-to-depth ratio (L/t) allowed for stability (segment B), given the assigned value of the ratio between the in situ uniaxial compressive strength (σ_c) and the vertical stress (σ_v).

The following section describes some case studies of man-made underground cavities in soft calcarenites, either subjected to failure or stable, and the corresponding application of the FEM-based charts to evaluate the corresponding unstable or stable conditions as a function of the mechanical and geometrical parameters.

3. Application to case studies

In order to validate the proposed stability charts, six real cases of underground artificial cavities, including three affected by sinkhole failures in the past and three in stable conditions at present, are presented later; it should be noted that the choice of underground quarries to test, depends on the assumptions made in drawing up the graphs with regard to both geometric and mechanical characteristics of cavity. As concerns the geometric features, the cavity must have a (more or less) horizontal roof, with a horizontal ground level surface and, generally, a generic 2D section of rooms of cavity, must be able to be schematized in a rectangular shape, as that of the Figure 1. The presence of isolated pillars or internal walls between two adjacent rooms of quarry may represents a critical element for a correct schematization but it is always possible to incorporate such structural elements to evaluate stability conditions with reference to a longer section. From a mechanical point of view, it is necessary that the cavity is excavated in soft carbonate rocks without both particular systems of joints or discontinuities (assumption of value of GSI = 100) and specific excavation techniques (i.e. use of explosives) that can alter stress state of rock involved (assumption of value of D = 0). The six presented cases well fit with the model's assumptions and, moreover, a detailed knowledge of sites (availability of maps and surveys for a correct reconstruction of the quarries) allowed the application of the stability charts.

3.1. Barletta sinkhole

In the night between 2 and 3 May of 2010, a large sinkhole occurred in the rural area of "San Procopio" (De Giovanni et al. 2011; Parise et al. 2013), near the town of Barletta (Apulia, southern Italy); the maximum diameter of the depression has been calculated to be approximately equal to 32 m at the ground surface (Figure 5).

Figure 5. Aerial view of the sinkhole occurred in the Barletta area.

Later on, geological and speleological surveys have revealed the existence of a complex network of artificial tunnels excavated presumably between the 19th and the 20th century in order to extract calcarenite rocks as a building material (De Giovanni et al. 2011; Parise et al. 2013). These studies have revealed that the underground cavity was formed of wide and long tunnels with a large number of isolated pillars showing an irregular spatial distribution, as reported in Figure 6a. In the sinkhole area (N-W sector of the cavity), the spatial distribution of pillars was coarsen, as compared with the rest of the cavity system, and characterised by the presence of only 8 pillars located at a

distance of about 10 ÷ 12 meters from the others; as such, these pillars were deemed to be heavily overloaded and probably subjected to high stress conditions.

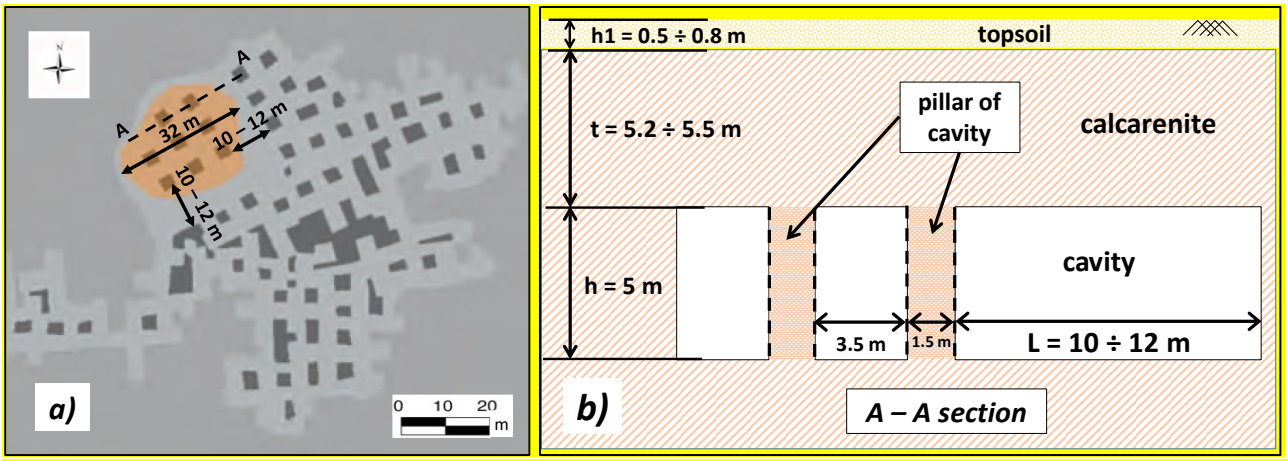

Figure 6. a) Schematic map of the Barletta underground calcarenite quarry (adapted after Luisi et al. 2015, the area involved in the collapse is shown in orange, pillars are in dark grey, and tunnels and excavated zones are in light grey); b) Original stratigraphy of the cavity (before collapse).

In order to detect the causes that led to the collapse of underground quarry, it should be note that instability evidences, as signs of pillar crushing or fractures with detachments from the vault and the walls (figure 7), were found throughout the cavity, especially close to the sinkhole area (De Giovanni et al. 2011). Therefore, starting from the original geometrical configuration of the cavity shown in Figure 6b, the loss of strength produced by the failure of the inner pillars, where high stress conditions are likely, may have generated an increase of the loading conditions for the whole roof, with the consequent generation of a sinkhole mechanism.

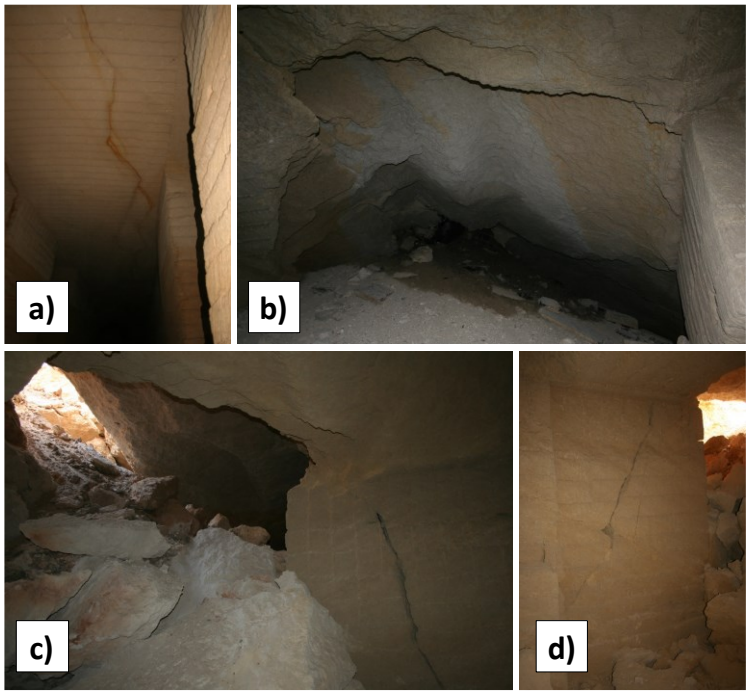

Figure 7. Instability evidences at the Barletta underground quarry: a) tensile fracturing of the vault; b) block detachment from the vault; c) open fractures on pillars, and vault collapses in the area closest to the sinkhole; d) crushing of pillar with joints (adapted after De Giovanni et al. 2011).

In order to verify the stability conditions using the charts proposed by Perrotti and co-authors (2018), an initial value of the cavity width of about 10 ÷ 12 meters, corresponding to the largest distance between two adjacent pillars (see Figure 6), has been assumed, bearing in mind that the failure of the nearby pillars has presumably implied an increase of the effective L parameter. Speleological surveys have indicated an average thickness of the calcarenite deposits in the study area of about 6 m, with minimum value of 4 m (De Giovanni et al., 2011), with an upper layer of about 0.5 ÷ 0.8 m composed of sandy-silty topsoil (unit weight γ = 20 kN/m^3) overlying a 5.2 ÷ 5.5 m thick calcarenite layer (γ = 17 kN/m^3). In the sinkhole area, the height of the cavity rooms has been generally measured to be about 5 m.

Uniaxial compression tests performed in the laboratory on calcarenite samples taken in the sinkhole area have indicated values of uniaxial compressive strength of about 1 ÷ 2 MPa under dry conditions and about 0,75 ÷ 1 MPa under saturated conditions (Luisi et al. 2015); tensile strength values derived from indirect tension tests have instead resulted to be approximately equal to 0.1 ÷ 0.2 MPa. Consequently, the parameter m_i to be used in the Hoek & Brown failure criterion results in a range between 6 and 11.

Hence, based on these evaluations, the non-dimensional ratios L/t and L/h can be estimated in the following ranges: 1.81 < L/t < 2.31 and 2 < L/h < 2.4.

The vertical stress at a depth of h=6m is estimated to be equal to:

$\sigma_v \approx (\gamma_{calc} \cdot t_{calc}) + (\gamma_{topsoil} \cdot h_{topsoil}) =$ 104.4 kPa

and, assuming σ_c = 1 MPa, a ratio σ_c/σ_v equal to about 9.6 is obtained.

In Table 2 the geometrical and the mechanical parameters, derived from speleological surveys and materials characterization, are reported; moreover, the values adopted for the application of the stability charts to the Barletta underground quarry are shown.

Geometrical and mechanical parameters from speleological surveys and material characterization				***Adopted values for stability charts application to Barletta cavity***			
L	10 ÷ 12	[m]		L / t	=	1.81 ÷ 2.31	[/]
t	5.2 ÷ 5.5	[m]					
h	5	[m]		L / h	=	2 ÷ 2.4	[/]
h1	0.5 ÷ 0.8	[m]	*topsoil*				
σ_c	1 ÷ 2	[MPa]	*(dry conditions)*	σ_c	=	1000	[kPa]
	0.75 ÷ 1		*(saturated conditions)*				
m_i	6 ÷ 11	[/]		m_i	=	8	[/]
γ	20	[kN/m^3]	*topsoil*	σ_v	=	104.4	[kPa]
	17		*calcarenite*	σ_c/σ_v	=	9.6	[/]

Table 2. Geometrical and mechanical parameters and adopted values for stability charts application to the Barletta underground quarry.

Therefore, considering the chart corresponding to a value $m_i = 8$ (Figure 3), and specifically the curve corresponding to L/h ratio between 2 and 3, in the initial conditions (unfailed pillars) the cavity results to be in the stability zone (Figure 8); however, if a strength loss of the nearby pillars is accounted for, an increase of the L representative parameter leads to a gradual increase of the ratio L/t (as well as of L/h ratio), with the consequent decrease of the safety margin until reaching the threshold curve corresponding to the L/h value (Figure 8), thus indicating failure conditions.

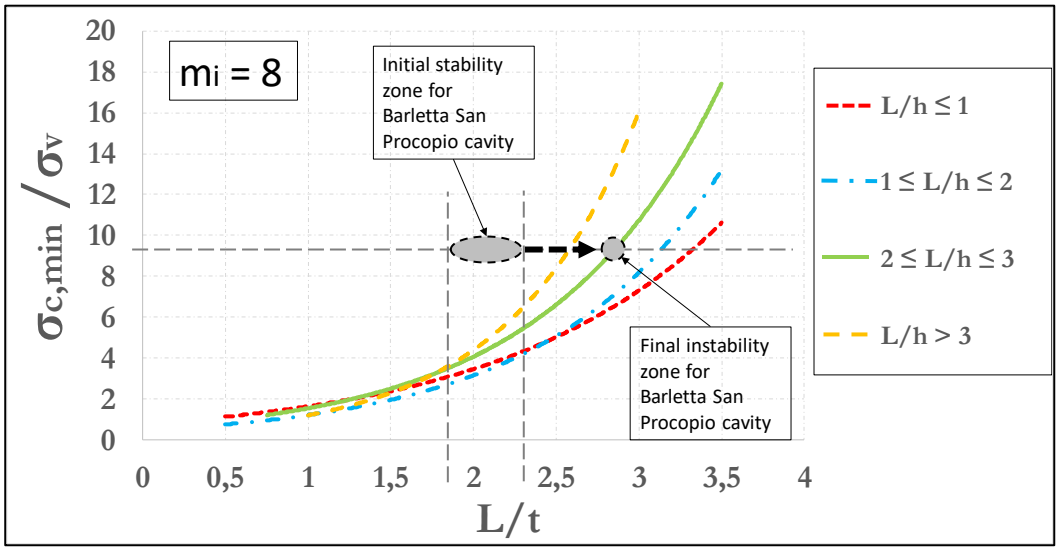

Figure 8. Application of stability chart (m_i=8) for the Barletta case study.

Figure 8 also shows that the cavity is close to failure conditions, already for values of ratio L/t larger than 2.75; therefore, even with the loss of the strength provided by a single pillar, a ratio L/t corresponding to the achievement of the threshold stability conditions follows.

3.2. Marsala sinkhole

A sinkhole took place in the town of Marsala (Sicily, Italy) in June 2011 in the area where underground quarries were excavated according to the room-and-pillar technique at depths ranging from 3 ÷ 4 meters to about 15 m; after the quarry abandonment, since the 1960's, the cavity has been progressively subjected to instability phenomena, represented by deformations and block detachments from the vaults and the pillars.

A detailed map of the underground cavity luckily existed before the collapse, thanks to speleological survey carried out in 2000 (Vattano et al. 2013). This allowed to properly map the sinkhole boundary above the underground quarry; with a minimum diameter of about 25 ÷ 30 m at the ground level, the sinkhole is shown in Figure 9. The figure shows that the examined quarry consists of rooms with quadrangular shape, in most cases connected and/or separated by thin rock walls or pillars. As specifically concerns the sinkhole area, the excavation was carried out according to an irregular scheme, leaving very small pillars and slight internal walls; larger sizes of the internal supporting elements, as well as lower room spans, are instead observed in the rest of the cavity system. The average room height has been estimated to be equal to 2.7 m, with the roof thickness varying from 8.2 to 11.8 m.

Figure 9. Plan of the Marsala underground quarry, with indication of the sinkhole area (adapted after Vattano et al. 2013).

For this study, Fazio et al. (2017) have proposed a three-dimensional finite element back-analysis and have found that the weakness of these overstressed internal structural elements could have been the reason for initial local failure, and then for global failure. In particular, the collapse of the pillars and the internal walls (very thin along A-A section of Figure 9) could have progressively entailed an increase in the width of the open galleries, leading to a total length, L, approximately equal to that of the sinkhole (D ≈ 25 ÷ 30m, Figure 9). Local failures of pillars and thin walls, as well as detachments and fracturing processes of the vault, are widely diffuse within the Marsala cavity, as documented in Figure 10 (Bonamini et. al, 2013).

The calcarenites outcropping in the study area can be schematised according to two lithotypes, with a top layer (thickness in a range between 8.2 ÷ 11.8 m) characterised by poor mechanical properties, and a stiffer deeper layer (Fazio et al. 2017); in figure 11 is reported the stratigraphy traced along A-A section of Figure 9.

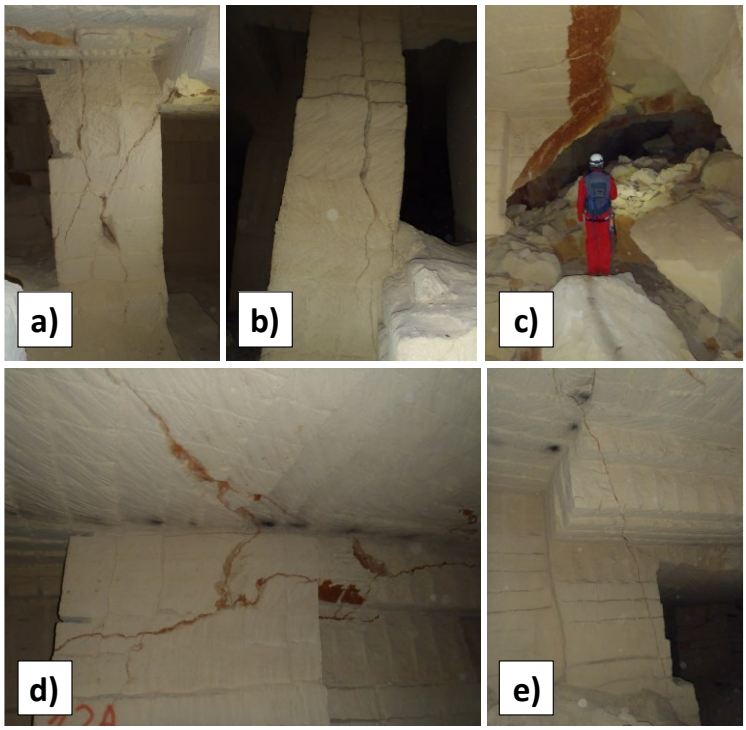

Figure 10. Instability evidences at the Marsala underground quarry: a) fracturing of a pillar; b) bending and failure of a pillar; c) material detachments from the vault; d) and e) diffuse fracturing within the walls and the vaults (Bonamini et. al, 2013).

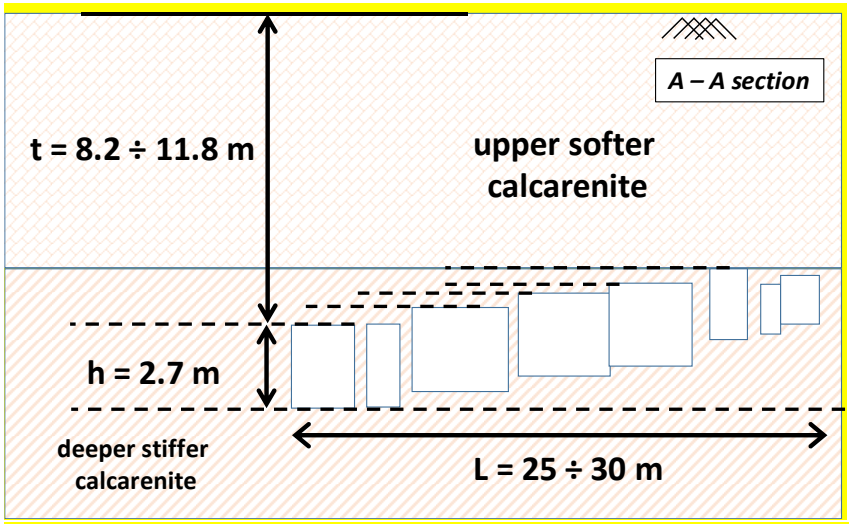

Figure 11. Stratigraphy of Marsala underground quarry traced along A-A section.

For the upper softer lithotype the dry unit weight is measured in the range between 12 and 15 kN/m^3, whereas the same parameter under saturated condition is between 13.5 and 17 kN/m^3. Uniaxial compressive strength under saturated conditions has been measured to reach about σ_c = 1.3 ÷ 1.6 MPa, whereas, with a saturation degree equal to zero, σ_c = 2 ÷ 3 MPa. The value of the tensile strength can be assumed to be 1/8 ÷ 1/10 of the compressive strength, in accordance with experimental works on similar calcarenite rocks (Andriani and Walsh 2010; Ciantia et al. 2015b), so that the m_i parameter to be used in the Hoek & Brown strength criterion results to be in a range between 8 and 10.

Based on the aforementioned parameters, considering a cavity width L ≈ 25 ÷ 30 m (corresponding to the collapse of internal pillars and walls in Figure 9), an average height h of 2.7 m and an average overburden thickness, t, of 10 m, the corresponding non-dimensional ratios L/t and L/h result to be in the following ranges: 2.5 < L/t < 3 and 9.2 < L/h < 11.1.

If a unit weight value γ_{calc} of 16 kN/m^3 is assumed, the vertical stress at depth of t = 10 m is equal to: $\sigma_v \approx (\gamma_{calc} \cdot t_{calc}) = 160$ kPa. Finally, assuming $\sigma_c = 2$ MPa (corresponding to an intermediate value between saturated and dry conditions), a ratio σ_c/σ_v approximately equal to 12.5 is obtained.

In Table 3 the geometrical and the mechanical parameters, derived from speleological surveys and materials characterization, are reported; moreover, the values adopted for the application of the stability charts to the Marsala underground quarry are shown.

Geometrical and mechanical parameters from speleological surveys and material characterization				***Adopted values for stability charts application to Marsala cavity***			
L	25 ÷ 30	[m]		t	=	10	[m]
t	8.2 ÷ 11.8	[m]		L / t	=	2.5 ÷ 3	[/]
h	2.7	[m]		L / h	=	9.2 ÷ 11.1	[/]
σ_c	2 ÷ 3	[MPa]	*(dry conditions)*	σ_c	=	2000	[kPa]
	1.3 ÷ 1.6		*(saturated conditions)*	γ	=	16	[kN/m^3]
m_i	8 ÷ 10	[/]		m_i	=	8	[/]
γ	13.5 ÷ 17	[kN/m^3]	*(dry conditions)*	σ_v	=	160	[kPa]
	12 ÷ 15		*(saturated conditions)*	σ_c/σ_v	=	12.5	[/]

Table 3. Geometrical and mechanical parameters and adopted values for stability charts application to the Marsala underground quarry.

Figure 12 shows the representative state of the Marsala cavity stability in the stability chart corresponding to $m_i = 8$. The figure indicates that the state is located on the curve characterized by L/h > 3 and this confirms the unstable condition of the underground quarry.

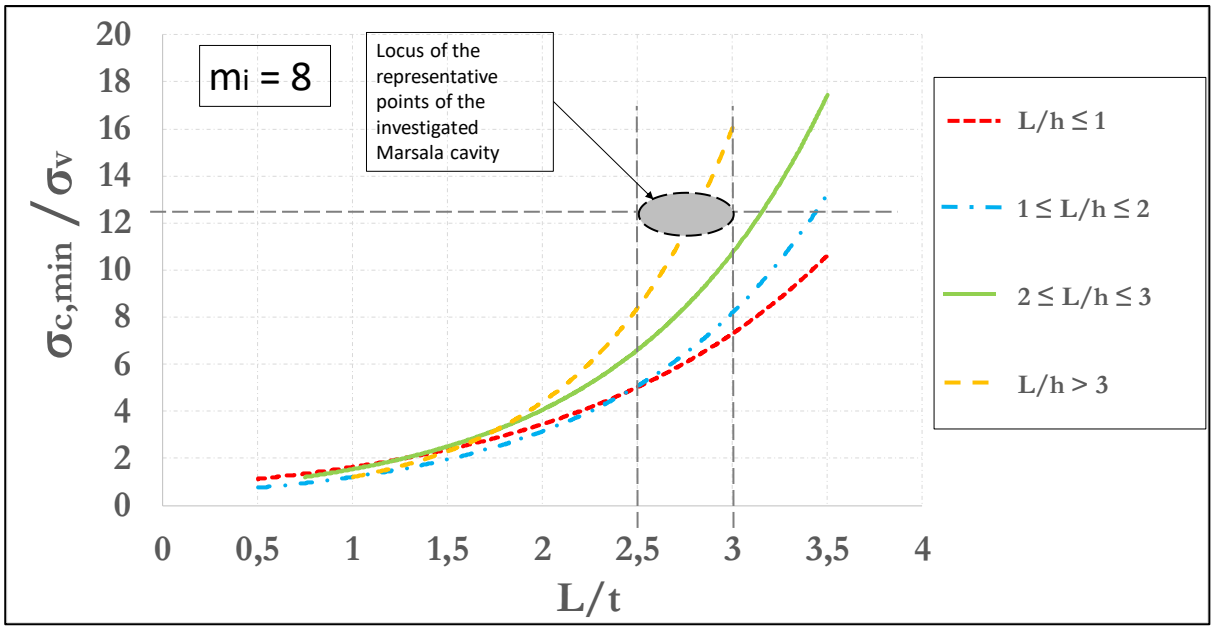

Figure 12. Application of stability chart (m_i = 8) for the Marsala underground quarry.

3.3. Gallipoli sinkhole

In the eastern urban area of the town of Gallipoli (southern Apulia) a large sinkhole occurred in 2007, between 29th March and 1st April, with the opening of a sub elliptical 12 m x 18 m chasm (Figure 13a), followed by a significant widening of the subsidence area at the ground level (Figure 13b) which affected some buildings located nearby.

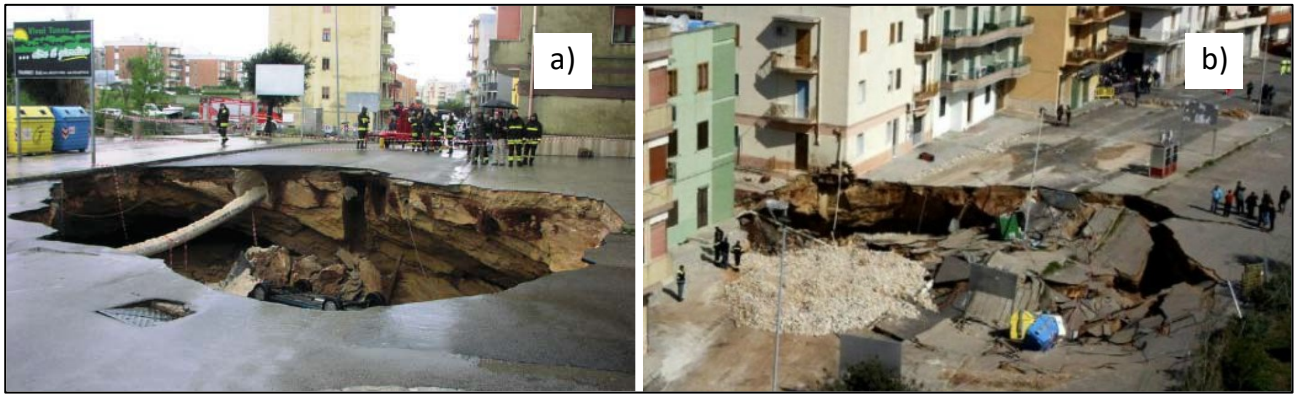

Figure 13. Pictures of the 2007 Gallipoli sinkhole: a) the first sinkhole as appeared in 29th March; b) enlargement of the chasm on 1st April.

Geological surveys performed soon after the collapse detected the existence of a complex underground cavity net, on a single level; although a room-and-pillar excavation technique was adopted, the resulting geometry of the cavity system is highly irregular, with rooms located at variable depth from the ground level: in particular, in the area where sinkhole occurred, the depth of the cave bottom is of about 8 m, with a roof thickness of less than 3 ÷ 4 meters. Moreover, diffuse signs of local instability, as block detachments from the vault and the lateral walls, debris heaps on the floor and fractures of pillars due to crushing were found within the cavity rooms (Delle Rose 2007; Parise 2012). Some of these local instabilities are shown in Figure 14.

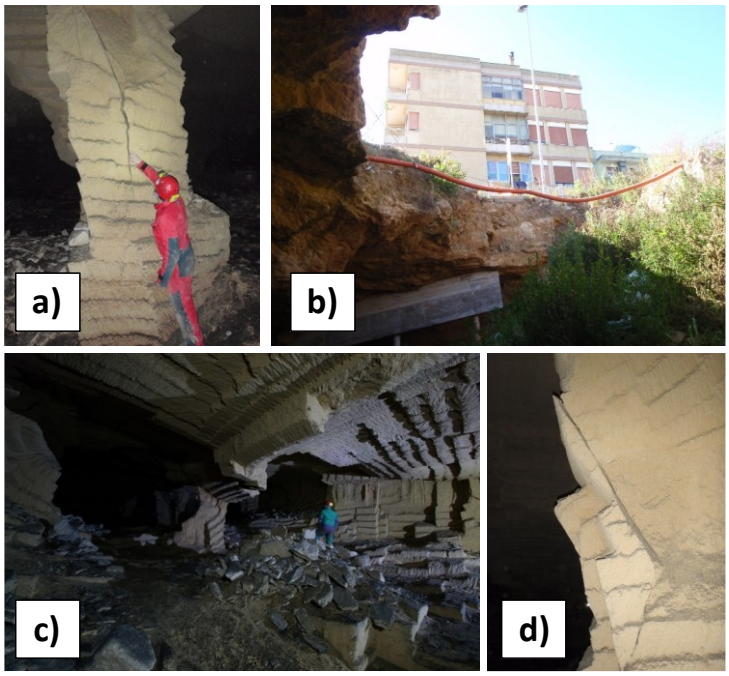

Figure 14. Evidences of instability at the Gallipoli underground quarry: a) extensive fracturing in a pillar; b) view of sinkhole from the bottom; c) inner view of one of the longest rooms in the cavity (block detachments from the vault and debris heaps on the floor); d) incipient block detachment from a pillar.

Based on the investigations performed, a reconstruction of the cavity geometry, before the collapse, has been carried out. Figure 15 shows the position of the remaining pillars, the zones with the accumulation of debris or detachments of blocks and the detailed perimeter of the sinkhole, for both the first collapse and the subsequent enlargement. The buildings and the roads on the ground surface overlying the area are also shown in the map.

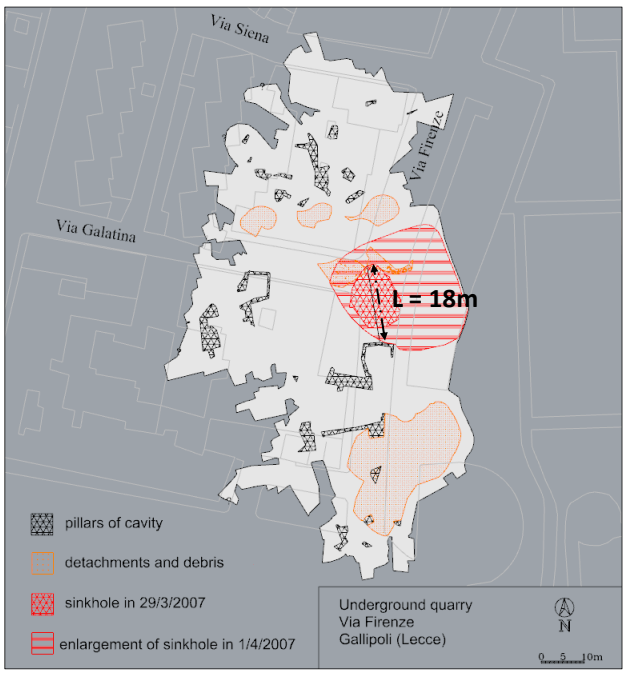

Figure 15. Map of the underground quarry in Via Firenze, Gallipoli, and overlying built environment.

In the sinkhole area, deposits of the Salento Calcarenites, consisting of alternations of calcarenite rocks and looser sediments, crop out; the rock volumes affected by the mining activity (i.e., the calcarenite) appear to be massive, whereas the upper layer, forming the cavity roof, is formed of laminated and stratified calcarenite deposits with very low mechanical properties (Delle Rose 2007; Parise 2012). Based on the saturation degree, uniaxial compressive strength σ_c results in a range between 2.5 and 3 MPa for dry samples and 1.7 ÷ 2.3 MPa for saturated rock (Ciantia et al. 2015). Tensile strength is variable between 0.7 and 1 MPa both in dry and saturated conditions, so that a parameter m_i = 3 ÷ 4 of the Hoek & Brown failure criterion has been derived accordingly. A unit weight about equal to 17.5 kN/m^3 has been also assumed.

As concerns the application of the stability charts to the Gallipoli case study, a cave width L of about 18 m (Figure 15) between two adjacent pillars is considered. The section trace along L is reported in Figure 16; the overburden thickness is assumed to be t = 3 ÷ 4 m and the height of cavity is h = 4 ÷ 5 m, so that the non-dimensional ratios L/t and L/h are in the following ranges: 4.5 < L/t < 6 and 3.6 < L/h < 4.5.

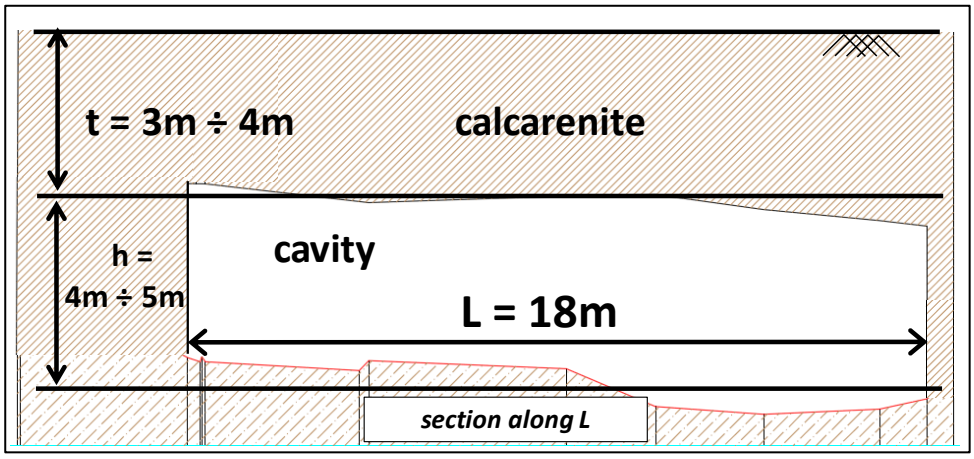

Figure 16. Cross-section of the failed cavity in Gallipoli.

The cavity roof is composed almost entirely by the upper calcarenite layers with lower mechanical properties, so that a value of σ_c = 2.7 MPa can be assumed. The vertical stress at the depth of h = 3 ÷ 4 m results to be:

$\sigma_v \approx (\gamma_{calc} \cdot t_{calc})$ = 52.5 ÷ 70 kPa;

and, consequently, the ratio σ_c/σ_v is in the range 38.6 ÷ 51.3.

In Table 4 the geometrical and the mechanical parameters, derived from speleological surveys and materials characterization, are reported; moreover, the values adopted for the application of the stability charts to the Gallipoli underground quarry are shown.

Geometrical and mechanical parameters from speleological surveys and material characterization				Adopted values for stability charts application to Gallipoli cavity			
L	18	[m]		L / t	=	4.5 ÷ 6	[/]
t	3 ÷ 4	[m]		L / h	=	3.6 ÷ 4.5	[/]
h	4 ÷ 5	[m]		σ_c	=	2700	[kPa]
σ_c	2.5 ÷ 3	[MPa]	*(dry conditions)*	γ	=	17.5	[kN/m^3]
	1.7 ÷ 2.3		*(saturated conditions)*	m_i	=	3	[/]
m_i	3 ÷ 4	[/]		σ_v	=	52.5 ÷ 70	[kPa]
γ	17.5	[kN/m^3]	*calcarenite*	σ_c/σ_v	=	38.6 ÷ 51.3	[/]

Table 4. Geometrical and mechanical parameters and adopted values for stability charts application to the Gallipoli underground quarry.

Taking into account the stability charts corresponding to $m_i = 3$ and, specifically, the threshold curve for L/h > 3, the representative area of the investigated cavity is very close to the threshold curve (Figure 17); therefore, it comes out that the cavity was in a state of incipient failure, so that some external factor, as for example vibrations or concentrated seepages, could have triggered the instability.

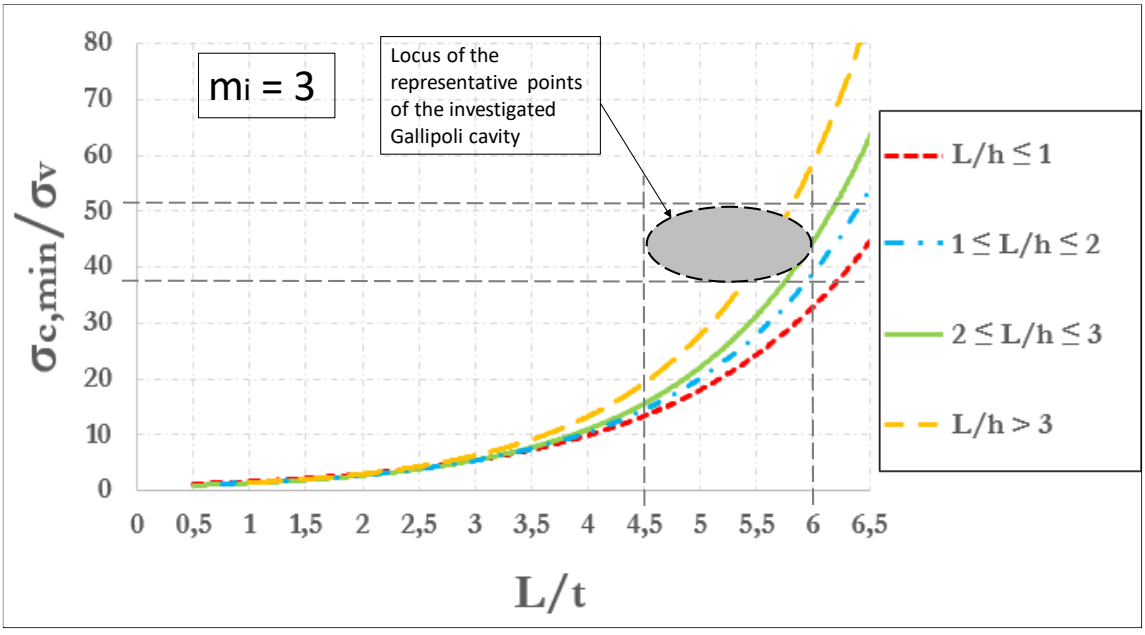

Figure 17. Application of stability chart ($m_i = 3$) for the Gallipoli underground quarry.

3.4. Cutrofiano underground caves

In the last century several underground quarries were excavated at the outskirts of the town of Cutrofiano (southern Apulia) with the room-and-pillar technique. Later on, these quarries were abandoned, and the urban area expanded above the areas originally interested by their development. Geological surveys have highlighted, in the southern part of the town, the existence of a diffuse net of underground cavities. The location of three quarries, respectively named as Cave A, Cave B and Cave C, with respect to the overlying built-up environment, is reported in Figure 18.

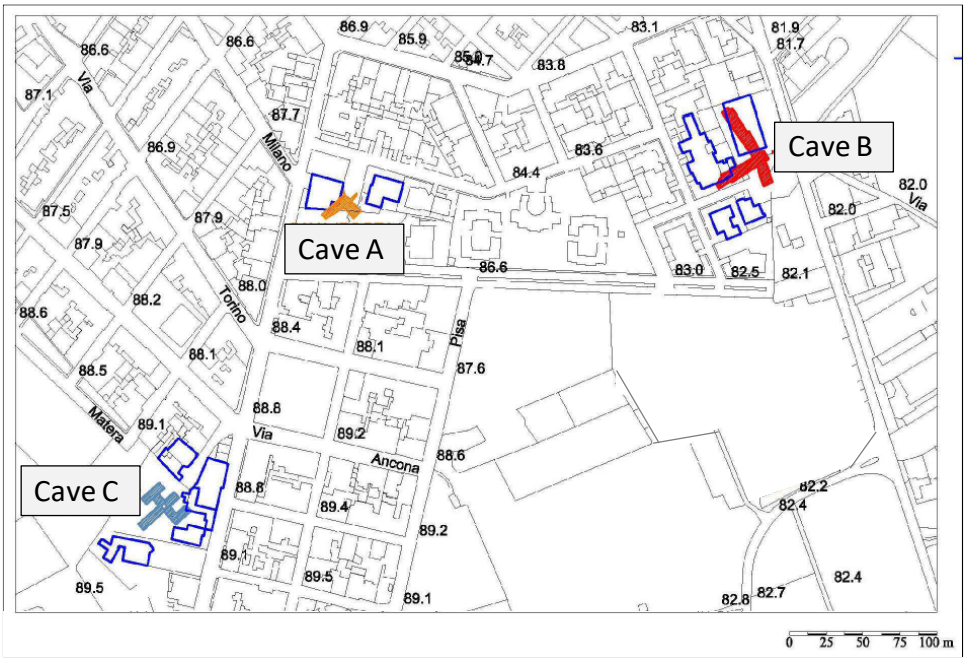

Figure 18. Location of the examined underground quarries at Cutrofiano.

All the three quarries give evidence of signs of local instability, as detachments of material from the walls and the vaults or pillar crushing that, frequently, represent prodromal signals of a possible general failure (Parise and Lollino 2011). Figure 19 highlights some of typical local failures detected in the Cutrofiano underground quarries.

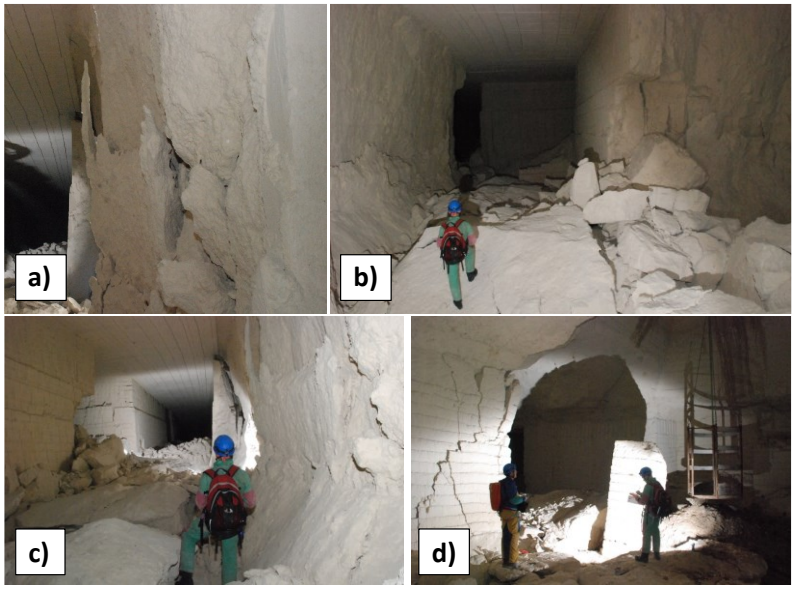

Figure 19. Signs of local instability in the Cutrofiano underground quarries: a) diffuse fracturing of a wall; b) detachments of material from walls; c) massive falls from the walls, with heavy production of debris heaps on the floor; d) open fractures at the pillars rim, in correspondence of the main shaft of access to the cavity.

For each of the examined cavities, a detailed geometrical and geological survey has been performed. The geological setup of the area is formed of shallow layers of clays, silts and/or sands that overlie a stiffer layer of calcarenite, locally named “Mazzaro”, which generally represent the roof of the quarries. Therefore, in order to apply the stability charts the “Mazzaro” level has been considered.

From a geomechanical point of view, unit weight values in the range of 18.6 ÷ 19.6 kN/m^3 for silty/sandy layers and 19.8 ÷ 20.5 kN/m^3 for the calcarenite layer has been respectively accounted for. A uniaxial compressive strength of about 2.4 MPa has been measured for the Mazzaro material forming the cave roofs (Lollino and Parise 2010), whereas the tensile strength is about 1/8 ÷ 1/10 of the compressive one, so that the parameter m_i of the Hoek & Brown failure criterion is assumed to be equal to m_i = 8÷10. In the following sub-sections, the representative conditions of each cavity are shown with respect to the corresponding chart.

3.4.1. Cave A

The stability analysis for cavity A has been carried out with reference to the cross-section AA in Figure 20. The width and height of cavity, are, respectively, equal to L = 7.50 m and h = 5.0 m, while the thickness of the resistant portion of the cave roof, which in this case is coincident with the "Mazzaro" rocky layer, is t = 4.30 m. Therefore, the non-dimensional ratios result to be about L/t ≈ 1.74 and L/h ≈ 1.5.

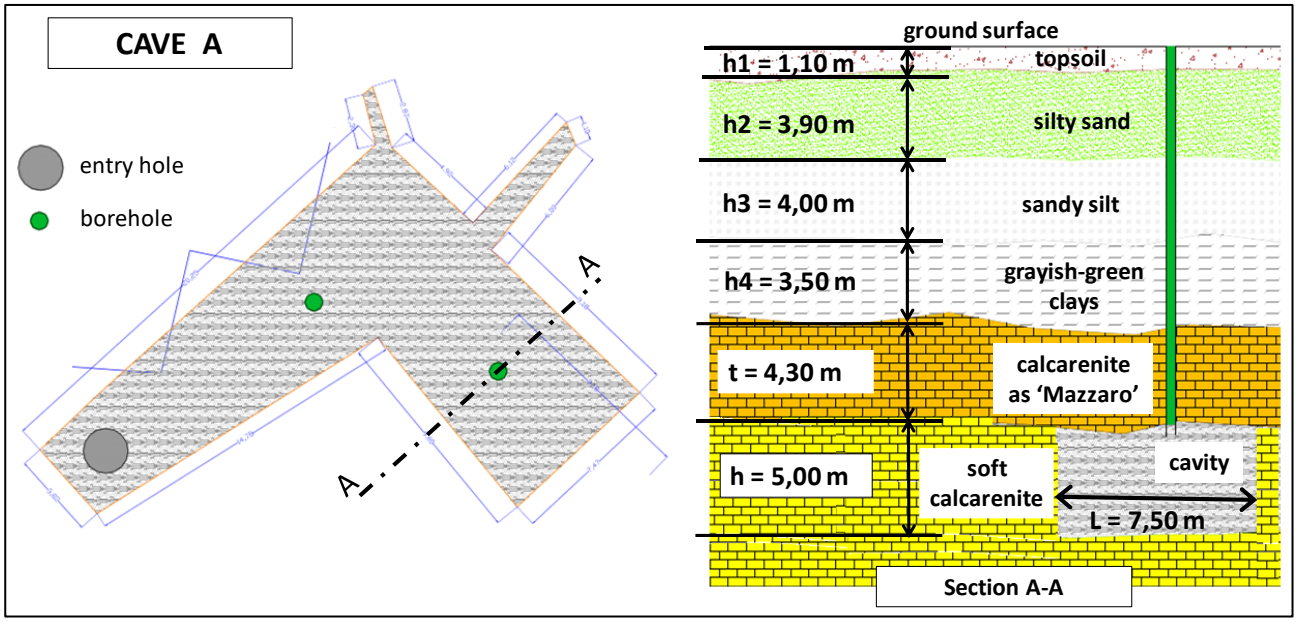

Figure 20. Plan and stratigraphy of the underground cavity A (adapted from Maglio and Ligori, 2014).

With reference to the stratigraphy in Figure 20, the vertical stress at the depth of the cavity roof is equal to:

$$\sigma_v \approx (\gamma_1 \cdot h_1) + (\gamma_2 \cdot h_2) + (\gamma_3 \cdot h_3) + (\gamma_4 \cdot h_4) + (\gamma \cdot t)_{mazzaro} = 324.82 \text{ kPa}$$

so that, if $\sigma_{c,min}$ = 2.4 MPa, we obtain an operative value of $\sigma_c/\sigma_v \approx 7.39$.

In Table 5 the geometrical and the mechanical parameters, derived from speleological surveys and materials characterization, are reported; moreover, the values adopted for the application of the stability charts to the Cutrofiano Cave A are shown.

Geometrical and mechanical parameters from speleological surveys and material characterization				Adopted values for stability charts application to Cutrofiano Cave A			
L	7.5	[m]	*cavity width*	L / t	=	1.74	[/]
t	4.3	[m]	*calcarenite thickness*	L / h	=	1.5	[/]
h	5	[m]	*cavity height*	γ	=	20.2	[kN/m^3]
h_1	1.1	[m]	*topsoil*	γ_1	=	19.6	[kN/m^3]
h_2	3.9	[m]	*silty sand layer*	γ_2	=	19	[kN/m^3]
h_3	4	[m]	*sandy silt layer*	γ_3	=	18.6	[kN/m^3]
h_4	3.5	[m]	*grayish-green clays layer*	γ_4	=	19.4	[kN/m^3]
σ_c	2.4	[MPa]	*average dry/saturated conditions*	σ_c	=	2400	[kPa]
m_i	8 ÷ 10	[/]		m_i	=	8	[/]
γ	19.8 ÷ 20.4	[kN/m^3]	*calcarenite*	σ_v	=	324.82	[kPa]
	18.6 ÷ 19.6		*silty/sandy/clay layers*	σ_c/σ_v	=	7.39	[/]

Table 5. Geometrical and mechanical parameters and adopted values for stability charts application to the underground Cutrofiano Cave A (Maglio and Ligori, 2014; Parise and Lollino,2010).

3.4.2. Cave B

For cave B the calculation has been performed for section B-B in Figure 21. It has to be noted that in this case a two story civil building exists just above the cavity, thus representing a further overburden stress, which has been approximately evaluated equal to q = 100 kPa.

The width and the height of the cavity are equal to L = 6.80 m and h = 5.00 m, respectively, while the thickness of the resistant beam-shaped portion of the roof, i.e. the “Mazzaro” layer, is t = 2.70 m. Therefore, the non-dimensional ratios result to be about L/t ≈ 2.52 and L/h ≈ 1.36.

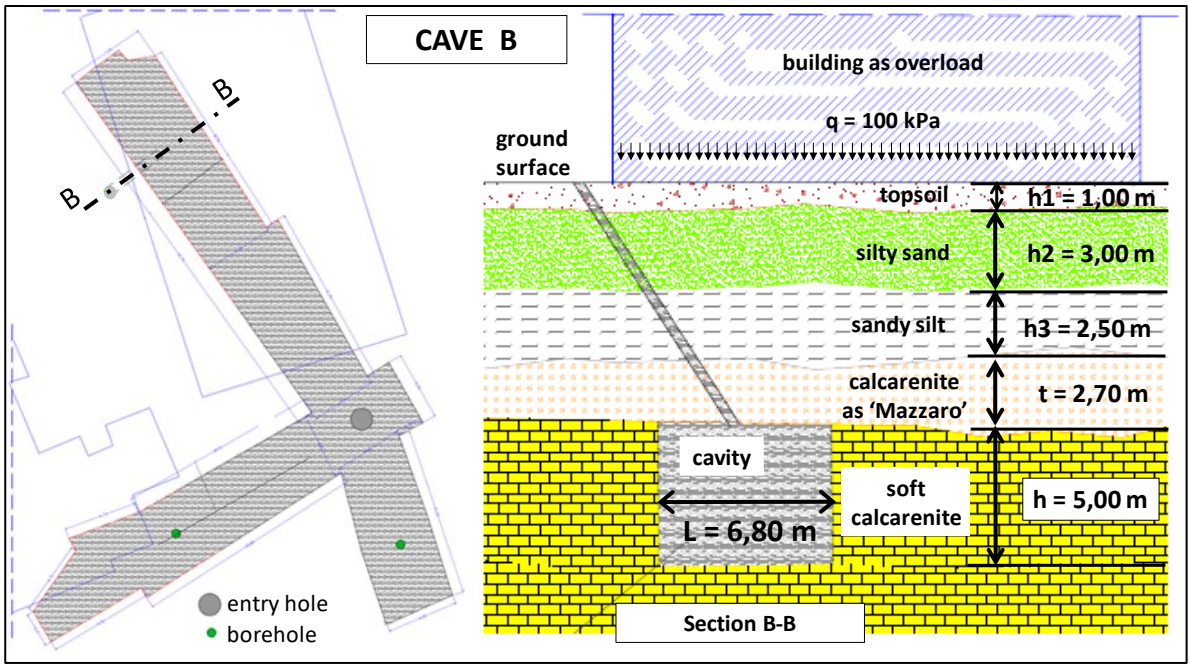

Figure 21. Plan and stratigraphy of the underground cavity B (adapted from Maglio and Ligori, 2014).

With reference to the stratigraphy in Figure 21, the vertical stress at the depth of the cavity roof is equal to:

$$\sigma_v \approx (\gamma_1 \cdot h_1) + (\gamma_2 \cdot h_2) + (\gamma_3 \cdot h_3) + (\gamma \cdot t)_{mazzaro} + q = 277.64 \text{ kPa}$$

So that, if σ_c = 2.4 MPa, the mobilized value of σ_c/σ_v is equal to 8.64.

In Table 6 the geometrical and the mechanical parameters, derived from speleological surveys and materials characterization, are reported; moreover, the values adopted for the application of the stability charts to the Cutrofiano Cave B are shown.

Geometrical and mechanical parameters from speleological surveys and material characterization				***Adopted values for stability charts application to Cutrofiano Cave B***			
L	6.8	[m]	*cavity width*	L / t	=	2.52	[/]
t	2.7	[m]	*calcarenite thickness*	L / h	=	1.36	[/]
h	5	[m]	*cavity height*	γ	=	20.2	[kN/m^3]
h_1	1	[m]	*topsoil*	γ_1	=	19.6	[kN/m^3]
h_2	3	[m]	*silty sand layer*	γ_2	=	19	[kN/m^3]
h_3	2.5	[m]	*sandy silt layer*	γ_3	=	18.6	[kN/m^3]
σ_c	2.4	[MPa]	*dry conditions*	σ_c	=	2400	[kPa]
m_i	8 ÷ 10	[/]		m_i	=	8	[/]
q	100	[kPa]	*overburden stress*	q	=	100	[kPa]
γ	19.8 ÷ 20.4	[kN/m^3]	*calcarenite*	σ_v	=	277.64	[kPa]
	18.6 ÷ 19.6		*silty/sandy/clay layers*	σ_c/σ_v	=	8.64	[/]

Table 6. Geometrical and mechanical parameters and adopted values for stability charts application to the underground Cutrofiano Cave B (Maglio and Ligori, 2014; Parise and Lollino,2010).

3.4.3. *Cave C*

For cave C the calculation has been performed for section C-C in Figure 22. The cave width and height are, respectively, equal to L = 5.50 m and h = 7.00 m, while the thickness of the resistant roof is t = 5.00 m and the corresponding non-dimensional ratios result about L/t ≈ 1.1 and L/h ≈ 0.8.

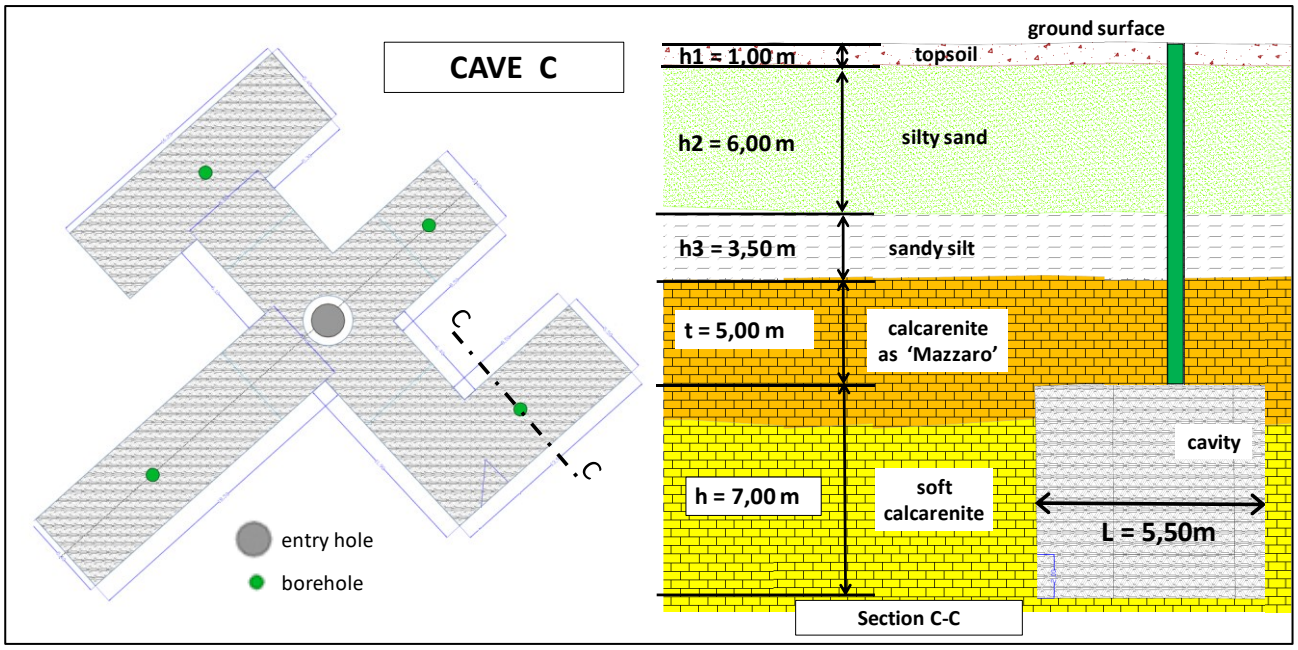

Figure 22. Plan and stratigraphy of the underground cavity C (adapted from Maglio and Ligori, 2014).

In this case, the vertical stress at the depth of the cavity roof results to be:

$$\sigma_v \approx (\gamma_1 \cdot h_1) + (\gamma_2 \cdot h_2) + (\gamma_3 \cdot h_3) + (\gamma \cdot t)_{Mazzaro} = 299.7 \text{ kPa}$$

and assuming $\sigma_c = 2.4$ MPa, we obtain $\sigma_c/\sigma_v \approx 8$.

In Table 7 the geometrical and the mechanical parameters, derived from speleological surveys and materials characterization, are reported; moreover, the values adopted for the application of the stability charts to the Cutrofiano Cave C are shown.

Geometrical and mechanical parameters from speleological surveys and material characterization				Adopted values for stability charts application to Cutrofiano Cave C			
L	5.5	[m]	*cavity width*	L / t	=	1.1	[/]
t	5	[m]	*calcarenite thickness*	L / h	=	0.8	[/]
h	7	[m]	*cavity height*	γ	=	20.2	[kN/m^3]
h_1	1	[m]	*topsoil*	γ_1		19.6	[kN/m^3]
h_2	6	[m]	*silty sand layer*	γ_2		19	[kN/m^3]
h_3	3.5	[m]	*sandy silt layer*	γ_3		18.6	[kN/m^3]
σ_c	2.4	[MPa]	*dry conditions*	σ_c	=	2400	[kPa]
m_i	8 ÷ 10	[/]		m_i	=	8	[/]
γ	19.8 ÷ 20.4	[kN/m^3]	*calcarenite*	σ_v	=	299.7	[kPa]
	18.6 ÷ 19.6		*silty/sandy/clay layers*	σ_c/σ_v	=	8	[/]

Table 7. Geometrical and mechanical parameters and adopted values for stability charts application to the underground Cutrofiano Cave C (Maglio and Ligori, 2014; Parise and Lollino,2010).

3.4.4. Application of stability chart (mi=8) to the three underground quarries at Cutrofiano

With calculated values of ratios L/t and σ_c/σ_v is possible, for the three caves A, B and C of Cutrofiano, to apply stability chart with value of m_i=8 as shown in Figure 23. Based on the L/h estimated ratios, Cave A and Cave B result to verify taking into account the light blue curve (1 ≤ L/h ≤ 2); for Cave C the corresponding curve in the graph is reported in red color (L/h ≤ 1).

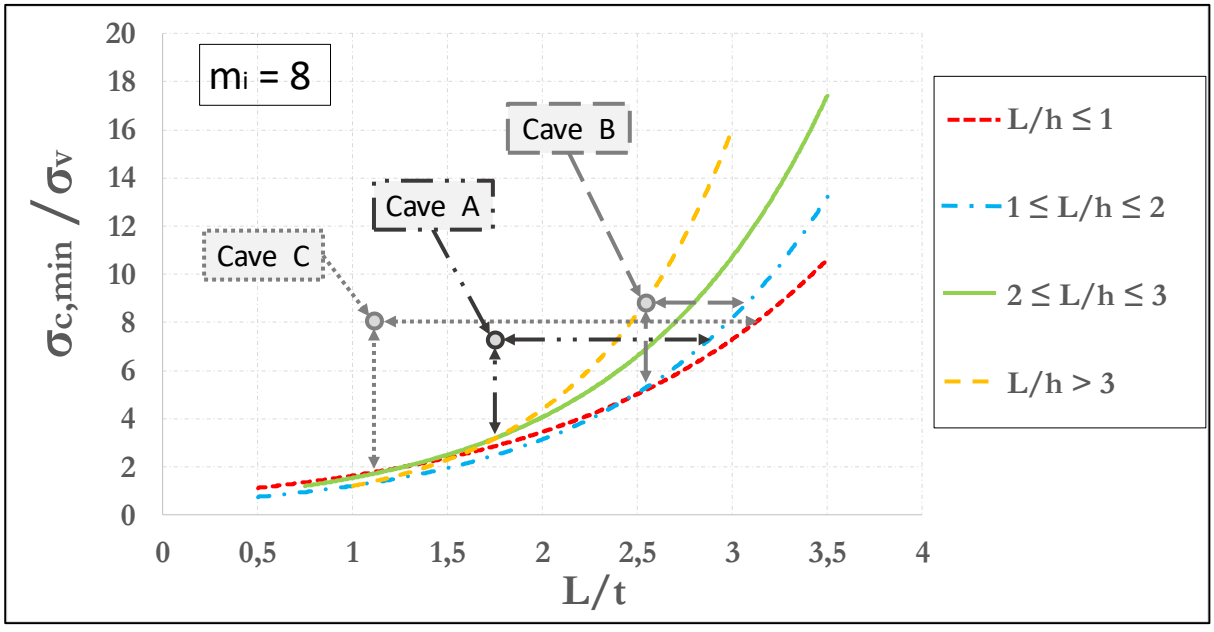

Figure 23. Application of the stability chart (m_i = 8) to the three underground quarries at Cutrofiano.

It can be pointed out that all the three cavities are in the stable zone of the chart of Figure 23, although with different safety margins; in fact, the margin of safety for Cave B is low, even for the presence of the overlying building. Cave A and cave C seem to be the most stable, also in relation to the geometry of the caves as well as to the thickness of the "Mazzaro" resistant layer.

4. Discussion and concluding remarks

In this paper, in order to validate the efficacy of the stability charts of Perrotti et al. (2018), six case studies of underground artificial cavities, including three affected by sinkhole failures in the past and three in stable conditions at present, have been presented. Practical application of graphs to real case studies is essential to assess the goodness of previous results; from this point of view, the proposed stability charts seem to be a valid method to evaluate the stability of underground cavities in soft carbonate rocks. The study of sinkholes is generally very complex, due to both the problem of reconstructing the geometric scheme before failure, and to the difficulties in identifying the corresponding triggering factors. Moreover, these types of failure occur for abandoned cavities for which a detailed geometry is typically not available (the Marsala case, here presented, was an exception to this rule). Nevertheless, post-failure in situ surveys can help in this task and bring out, especially, what are the most likely causes leading to collapse.

For the Barletta and Marsala sinkhole case studies, the failure of the underground cave highlighted the vulnerability of the internal supporting elements, as singular pillars, on the entire system of quarry: as such, the loss of material strength with time, due to weathering effects, could lead to local instabilities, as detachments of rocks from the pillars, and, consequently, a reduction of the resistant cross-section that, in the long term, could result in a general pillar crushing. If the surrounding pillars are not able to sustain the stresses redistributed due to the previous instabilities, a progressive failure process of the internal pillars is likely to occur. This, in turn, leads to the increase of the distance between supporting elements, i.e. the cavity width, and therefore the possible general failure of the whole cave, with development of a sinkhole (generally, of the collapse or cover collapse types; Gutierrez et al. 2014). Similarly, as well as the pillars, even the partition walls can also represent weakness elements of the system, especially when they are thin. Typically, soft and very soft rocks are exposed at a natural process of degradation (mainly due to the weathering effects with cyclical and seasonal fluctuations of water content) that may accelerate when overloads induced by underground works or vehicular traffic are applied. In an incipient state of collapse, such as that found in the stability chart of the Gallipoli underground quarry, low rates of vibrations could lead toward an acceleration of crack tensile opening with, consequently, propagation of fractures and formation of a sinkhole.

When underground quarries are suitably surveyed and mapped, a quantitative assessment of the stability conditions is possible; from this point of view, as shown for the three cases of underground quarries at Cutrofiano, stability charts allow preliminarily to evaluate the risk of an incipient collapse. For all the Cutrofiano case studies, stability charts have been applied for the section where the ratio L/t is the biggest within the cavity, in order to consider the most dangerous area in terms of safety: they resulted in stable conditions, even though with different safety margins. Furthermore, using stability charts is possible, within the same cavity, to distinguish the areas more susceptible to instability phenomena. Based on these evaluations, the management of underground quarries may change according to the evolution of the corresponding stability conditions.

It is important to highlight once again that the use of stability charts is limited to the stage of preliminary analysis. This means that such charts, especially when built upon a very high number of cases, could be extremely useful to technicians and practitioners for a first evaluation of the stability conditions. However, in case a proneness to collapse is ascertained through the stability chart, it is

493 absolutely necessary to move to the next stage, by carrying out site-specific tests and geotechnical
494 laboratory tests on rock samples for the determination of the parameters needed for a full analysis
495 of stability. The main limit of such an approach is therefore represented by an erroneous use of the
496 charts, with the wrong belief that they could act as substitute to in situ and laboratory tests.
497 Notwithstanding such drawback, the approach here presented can definitely be of help, especially
498 when a high number of cavities need to be initially assessed, as concerns the stability standpoint.

499 **References**

500 Andriani, G.F., Walsh, N. Petrophysical and mechanical properties of soft and porous building rocks
501 used in apulian monuments (South Italy). Geol. Soc., London, Spec. Publ., 333, 129–141, 2010.

502 Bonamini, M., Di Maggio, C., Lollino, P., Madonia, G., Parise, M., Vattano, M.. Sprofondamenti di
503 origine antropica nell'area di Marsala (Sicilia occidentale) analizzati mediante rilievi in sito e analisi
504 numerica dei processi di instabilità nelle cave sotterranee. Mem. Descr. Carta Geol. d'It. 93, 105–
505 120, 2013.

506 Cai, M. Practical estimates of tensile strength and Hoek–Brown strength parameter mi of brittle
507 rocks. Rock Mech. Rock Eng., 43(2), 167–184, 2010.

508 Carter, T.G. Guidelines for use of the scaled span method for surface crown pillar stability
509 assessment Ontario Ministry of Northern Development and Mines, 2010, pp. 1–34, 2014.

510 Castellanza, R., Lollino, P., Ciantia, M.O. A methodological approach to assess the hazard of
511 underground cavities subjected to environmental weathering. Tunnelling and Underground Space
512 Technology 82:278-292. Elsevier. DOI: 10.1016/j.tust.2018.08.041, 2018.

513 Ciantia, M.O., Castellanza, R., Di Prisco, C. Experimental study on the water-induced weakening of
514 calcarenites. Rock Mech. Rock Eng., 48(2), 441–461, 2015.

515 Coviello, A., Lagioia, R., Nova, R. On the measurement of the tensile strength of soft rocks. Rock
516 Mech. Rock Eng., 38(4), 251–273, 2005.

517 De Giovanni, A., Martimucci, V., Marzulli, M., Parise, M., Pentimone, N., Sportelli, D. Operazioni di
518 rilievo e analisi preliminare dello sprofondamento in località San Procopio (Barletta) del 2-3 maggio
519 2010. Opera Ipogea, Journal of Speleology in Artificial Cavities, 1-2, pp. 151-158, 2011.

520 Delle Rose, M. La voragine di Gallipoli e le attività di protezione civile dell'IRPI-CNR. Geologi e
521 Territorio. n° 4-2006 / 1-2007 pp. 3-12, 2007.

522 Evangelista, A., Pellegrino, A., Viggiani, C. Cavità e gallerie nel Tufo Giallo Napoletano. Atti IX Ciclo
523 Conf. MIR, Le opera in sotterraneo e il rapporto con l'ambiente, Patron Editore. FALLA
524 CASTELFRANCHI M. (1991) Pittura monumentale bizantina in Puglia. Milan, Italy, 2003.

525 Fazio, N. L., Perrotti, M., Lollino, P., Parise, M., Vattano, M., Madonia, G., Di Maggio, C. A three-
526 dimensional back-analysis of the collapse of an underground cavity in soft rocks. Engineering
527 Geology, 228, 301-311, 2017.

528 Federico, F., Screpanti, S. Effects of filling shallow room and pillar mines in weak pyroclastic rock.
529 Proc., XIII European Conference on Soil Mechanics and Geotechnical Engineering, Geotechnical
530 Problems with Man-made and Man Influenced. Grounds, Prague, The Czech Republic, 2003.

531 Ferrero, A. M., Segalini, A., Giani, G. P. Stability analysis of historic underground quarries. Comput.
532 Geotech., 37(4), 476–486, 2010.

533 Fiore, A., Fazio, N. L., Lollino, P., Luisi, M., Miccoli, M. N., Pagliarulo, R., Perrotti, M., Pisano, L.,
534 Spalluto, L., Vennari, C., Vessia G., Parise, M. Evaluating the susceptibility to anthropogenic
535 sinkholes in Apulian calcarenites, southern Italy. Geological Society, London, Special
536 Publications, 466, 381-396, https://doi.org/10.1144/SP466.20, 2018.

537 Fiore, A., Parise, M. Cronologia degli eventi di sprofondamento in Puglia, con particolare riferimento
538 alle interazioni con l'ambiente antropizzato. Memorie Descrittive della Carta Geologica d'Italia, 93,
539 239-252, 2013.

540 Fraldi, M., Guarracino, F. Limit analysis of collapse mechanisms in cavities and tunnels according to
541 the Hoek–Brown failure criterion. Int. J. Rock Mech. Min. Sci., 46(4), 665–673, 2009.

542 Gesualdo, A., Minutolo, V., and Nunziante, L. Failure in Mohr–Coulomb soil cavities. Can. Geotech.
543 J., 38(6), 1314–1320, 2001.

544 Goodings, D. J., Abdulla, W. A. Stability charts for predicting sinkholes in weakly cemented sand over
545 karst limestone. Eng. Geol., 65(2–3), 179–184, 2002.

546 Gutierrez, F., Parise, M., De Waele, L., Jourde, H. A review on natural and human-induced
547 geohazards and impacts in karst. Earth Science Reviews, 138, 61-88, 2014.

548 Hoek, E. Strength of rock and rock masses. News J. ISRM, 2(2), 4–16, 1994.

549 Hoek E. Practical rock engineering.
550 (https://www.rocscience.com/documents/hoek/corner/Practical-Rock-Engineering-Full-Text.pdf),
551 2007.

552 Hoek, E., Brown, E. T. Practical estimates of rock mass strength. Int. J. Rock Mech. Min. Sci., 34(8),
553 1165–1186, 1997.

554 Hoek, E., Martin, C. D. Fracture initiation and propagation in intact rock–A review. J. Rock Mech.
555 Geotech. Eng., 6(4), 287–300, 2014.

556 Lollino, P., Parise, M. Analisi numerica di processi di instabilità di cavità sotterranee e degli effetti
557 indotti in superficie. Proc. 2nd Int. Workshop "I sinkholes. Gli sprofondamenti catastrofici
558 nell'ambiente naturale ed in quello antropizzato", Rome, 3-4 December 2009, 803.816, 2010.

559 Luisi, M., Di Santo, A., Fiore, A., Lepore, D., Lollino, P., Miccoli, M.N., Parise, M., Spalluto, L.
560 Modellazione numerica 3D agli elementi finiti (FEM) per la valutazione delle condizioni di stabilità
561 di cavità antropiche del territorio pugliese: il caso studio della cava ipogea di San Procopio (Barletta,
562 Murge settentrionali). Mem. Descr. Carta Geol. d'It. XCIX, 327 – 336, 2015.

563 Maglio, A., Ligori, F. Intervento di bonifica e messa in sicurezza di cavità antropiche presenti nell'area
564 urbana e suburbana. Studio di prefattibilità ambientale Maggio 2014. Comune di Cutrofiano.
565 Ministero dell'Ambiente della Tutela del Territorio e del Mare, 2014.

566 Parise, M. The impacts of quarrying in the Apulian karst. In: CARRASCO, F., LA MOREAUX, J.W., DURAN
567 VALSERO, J.J., ANDREO, B. (eds.), Advances in research in karst media. Springer, p. 441-447, 2010.

568 Parise, M. A present risk from past activities: sinkhole occurrence above underground quarries.
569 Carbonates and Evaporites, 27 (2), 109-118, 2012.

570 Parise, M., Lollino, P. A preliminary analysis of failure mechanisms in karst and man-made
571 underground caves in Southern Italy. Geomorphology, 134(1–2), 132–143, 2011.

572 Parise, M., De Giovanni, A., Martimucci, V. Sinkholes caused by underground quarries: the case of
573 the 2–3 May 2010, event at Barletta (Southern Italy). Speleology and Spelestology, Proceedings IV
574 International Scientific Conference, November 2013, Nabereznye Chelny (Russia), 158-162, 2013.

575 Perrotti, M., Lollino, P., Fazio, N.L., Pisano, L., Vessia, G., Parise, M., Fiore, A., Luisi, M. Finite element-
576 based stability charts for underground cavities in soft calcarenites, International Journal of
577 Geomechanics, 10.1061/(ASCE)GM.1943-5622.0001175, 2018.

578 Suchowerska, A. M., Merifield, R. S., Carter, J. P., Clausen, J. “Prediction of underground cavity roof
579 collapse using the Hoek–Brown failure criterion.” Comput. Geotech., 44, 93–103, 2012.

580 Vattano, M., Di Maggio, C., Madonia, G., Parise, M., Lollino, P., Bonamini, M. Examples of
581 anthropogenic sinkholes in Sicily and comparison with similar phenomena in southern Italy. In: Proc.
582 13th Multidisc. Conf., May 6–10, Carlsbad, New Mexico. NCKRI Symposium, vol. 2. pp. 263–271,
583 2013.